Laminar Mixing in Different Interdigital Micromixers: II. Numerical Simulations

S. Hardt and F. Schönfeld
Institut für Mikrotechnik Mainz, 55129 Mainz, Germany

Flow patterns and mixing properties of micromixing devices described in Part I are investigated by computational fluid dynamics (CFD) and semianalytical methods. The CFD results provide qualitative information on mixing, but, due to numerical artifacts, no quantitative information can be derived in most cases. The geometrical arrangement of liquid lamellae predicted by the CFD simulations explain transmitted-light experiments reported in Part I. In contrast, the semianalytical method provides a simple model for the mixing devices presented and allows to assess their mixing properties. For two of the four micromixers, mixing times were in the range of milliseconds, thus lending themselves to fast, mass-transfer-limited reactions. Experimental data obtained for a specific micromixer support the semianalytical model. Both the model and experiments suggest that geometric focusing of a large number of liquid streams is a powerful micromixing principle.

Introduction

In recent years, the potential of microreactors for chemical process technology has been investigated in some detail (Ehrfeld et al., 1999). Apparent advantages of microreactors are enhanced heat and mass transfer due to high temperature and concentration gradients. An integral part of chemical process technology on the microscale are micromixers, which allow for fast and uniform mixing of fluids in the laminar regime under well-defined process conditions (Bessoth et al., 1999; Ehrfeld et al., 1999), as well as for dispersing immiscible fluids (Herweck et al., 2001). The mixing process of liquids in specially designed, transparent micromixers made of photostructurable glass was studied experimentally (Hessel et al., 2002). For this purpose, two different experimental techniques were developed and applied to four different mixer designs, which are termed rectangular, slit-shaped, triangular, and the SuperFocus mixer. The different mixer geometries, which share an interdigital arrangement of inlet streams as a common feature, are displayed in Figure 1. Details on the dimensions of the microstructures are reported in the experimental Part I of this article (Hessel et al., 2003). All the mixer designs, with the exception of the rectangular mixer, share the feature of "geometric focusing," that is, a narrowing of the flow cross section downstream of the inlet section.

Nowadays, methods of computational fluid dynamics (CFD) allow modeling of many flow phenomena in three dimensions with a high degree of accuracy. This opens up the possibility of proofing the feasibility of processes in microreaction devices or to optimize these devices on a computer with a minimum expenditure of time and money. In contrast to macroscopic mixers, which are typically operated under turbulent flow conditions, CFD simulations for micromixers can be based on a first-principle approach, without the need to em-

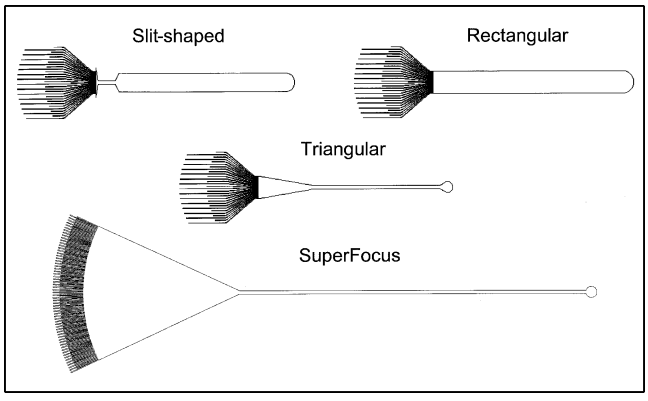

Figure 1. Micromixer designs.

Correspondence concerning this article should be addressed to S. Hardt.

ploy heuristic descriptions, as inherent in turbulence models. The purpose of this work is to give an overview on the flow patterns in micromixers, to demonstrate a few special approaches for modeling of these mixers, and to show the way to optimized mixer geometries. The starting point of the investigations are the mixer designs and experiments described in the experimental Part I of this article (Hessel et al., 2003).

CFD Simulations

A detailed comprehensive understanding of hydrodynamic aspects involved in the mixing processes is crucial, both for optimization of mixer designs and for a reliable interpretation of the experimental results.

In principle, information on flow and mixing can be obtained via a numerical solution of the Navier-Stokes equation and the convection-diffusion equation for the concentration field. The techniques commonly employed here are the finite-element (FEM) or the finite-volume method (FVM). However, numerical errors which are due to discretization of the convective terms in the transport equation of the concentration fields introduce an additional, unphysical diffusion mechanism (Noll, 1993). This so-called numerical diffusion (ND) is likely to dominate diffusive mass transfer on computational grids, especially for liquid-liquid mixing with characteristic diffusion constants in the order of 10^{-9} m^2/s. As an example, in a FVM discretization the numerical diffusion constant obtained with the popular UPWIND scheme is given by

$$\Gamma_{\text{num}} = \frac{u\Delta x}{2} \tag{1}$$

where ρ is the fluid density, u is its velocity, and Δx is the extension of a computational cell. Similar expressions can be applied to the y and z coordinate directions. With typical flow velocities within micromixers in the range of 1 m/s and typical computational grids, one obtains numerical diffusion constants much larger than the diffusion constants for liquid-liquid mixing.

There are a couple of measures to be taken in order to minimize ND. Higher-order discretization schemes as the QUICK scheme (Leonard, 1987) reduce the numerical errors. Furthermore, ND strongly depends on the relative orientation of flow velocity and grid cells (Noll, 1993). ND can be minimized by choosing grid cells with edges parallel to the local flow velocity.

The numerical results presented in this work are based on the solution of the incompressible Navier-Stokes equation

$$\frac{\partial u_i}{\partial t} + (u_j \cdot \nabla_j) u_i = -\frac{1}{\rho} \nabla_i p + \frac{\eta}{\rho} \nabla^2 u_i \tag{2}$$

the equation of mass conservation for incompressible fluids

$$\nabla_i u_i = 0 \tag{3}$$

and a convection-diffusion equation for the concentration field

$$\frac{\partial c}{\partial t} + (u_i \cdot \nabla_i) c = D\nabla^2 c \tag{4}$$

by means of the finite-volume method. u_i is the fluid velocity, ρ and η are its density and viscosity, D is the binary diffusion constant, and p and c denote density and concentration, respectively. For pressure-velocity coupling, the SIMPLEC algorithm (van Doormal and Raithby, 1984) was used. The simulations were done with the commercial flow solver CFX4 of AEA Technology.

In order to study numerical diffusion artifacts and possible remedies, the flow problem in the slit-shaped mixer was solved with a first-order upwind scheme for the concentration equation and with the third-order QUICK scheme. The results, obtained for a Reynolds (Re) number of 108 in the mixing channel, are shown in Figure 2. The flow rates assumed here represent characteristic operation parameters of micromixing devices. In order to make use of reflection symmetry, a geometry model was set up with 29 inlets (instead of 30) each having a width of 60 μm. The separating walls between the inlet channels have a width of 50 μm. The height of the channels and the mixing chamber is 150 μm. Only one-fourth of the actual geometry was modeled, thus exploiting the twofold symmetry. Furthermore, in order to keep the computational model as small as possible, only a minor section of the mixing channel was modeled. A body-fitted grid of almost 500,000 cells was used, which allows overnight runs on a standard workstation. In order to highlight the effects of numerical diffusion, the species diffusion constant was set to zero.

Two fluids, color-encoded in black and white, enter the mixing chamber where lamellae are formed and are subsequently focused. The concentration field on the lefthand side, of the figure was obtained with the QUICK scheme, whereas, for the results shown on the righthand side, the first-order upwind scheme was used. Obviously, the fluid lamellae are better resolved with the higher-order differencing scheme. However, both simulations show large gray regions, which have to be solely attributed to ND. These results show that, for the geometry and the Re number under study, a quantitative analysis of mixing processes is not possible within the chosen approach.

Qualitative information on the mixing process can be obtained by post-processing the simulation data for the concentration field. By proper adjustment of the gray scale, the contrast can be enhanced with respect to the results shown in Figure 2a. Furthermore, Figure 2b shows such contrast-enhanced images displaying the cross-section of the mixing channel at the outlet of the computational model for different Re numbers (the values of which were chosen to reproduce the volume flows of an experimental setup). The geometric arrangement and deformation of the liquid lamellae after focusing becomes visible. For low flow velocities, the fluid lamellae stay almost vertically aligned, whereas a u-shape is exhibited for larger Re. Going along with this deformation is a narrowing of the lamellae in the center and a broadening in certain regions.

In Figure 2c the lamellae profile for $Re = 108$ is displayed together with contour lines corresponding to constant values of the absolute flow velocity. The largest velocities occur in the center of the mixing channel. Hence, the corresponding fluid molecules experience the largest inertial forces towards the vertical symmetry plane after geometric focusing. This "inertial focusing" leads to the reduced lamellae widths observed in the central part. From Figure 2c, it becomes obvi-

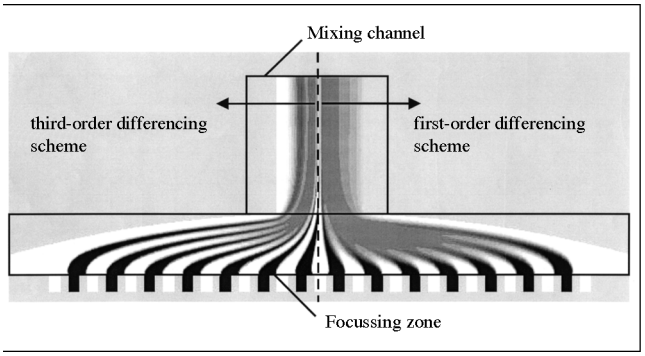

Figure 2a. Concentration field in the slit-shaped mixer obtained with a first-order upwind differencing (right) and third-order QUICK scheme (left).

ous that mixing is not uniform over the cross-sectional area of the channel: there are regions with comparatively thin lamellae and a low flow velocity together with regions of high flow velocity containing thicker lamellae. In the former, a high mixing quality is achieved, while in the latter poor mixing is observed.

The postprocessing technique described in the previous paragraph has its limitations, especially at high *Re* numbers. The method is limited by the graphical resolution of the hardware used and is strongly subjected to numerical noise, thus making it impossible to resolve fine and intertwined lamellae. However, without reference to concentration dynamics, the velocity distribution itself contains information which allows to qualitatively analyze the mixing process. The velocity field taken from the slit-mixer simulation was integrated for visualization of streamlines. In order to distinguish between different fluids, each streamline was assigned a unique color, depending on the inlet where the streamline enters the mixer geometry. This method reproduces the flow patterns of a binary liquid system with a diffusion constant

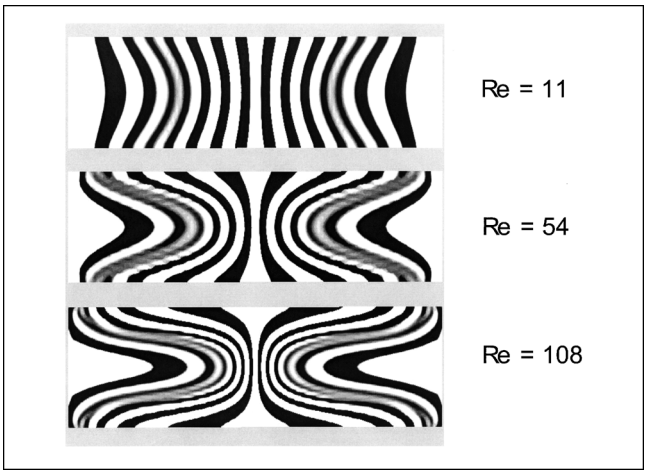

Figure 2b. Orientation of liquid lamellae in the mixing channel of the slit-shaped micromixer: viewing direction is the flow direction.

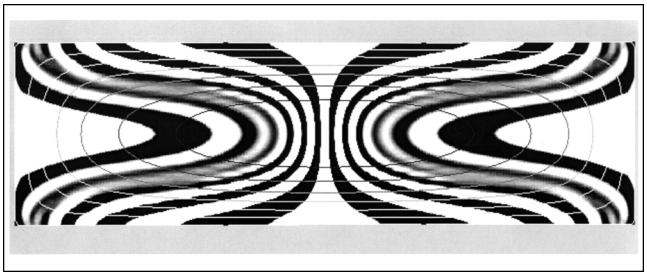

Figure 2c. Liquid lamellae and velocity contours in the mixing channel of the slit-shaped micromixer.

$D = 0$. At low *Re* numbers, when no recirculation is present, the full mixer domain is reconstructed by streamline tracking. At higher *Re* numbers, recirculation zones might emerge and the streamline tracking technique covers only a part of the mixer domain. The numerical solution of the velocity field and the integration algorithm for streamline tracking are still subject to discretization errors, but the actual problem of numerical diffusion is eliminated with this method.

Figure 2d shows the streamline pattern in the mixing channel of the slit-shaped mixer at $Re = 2{,}160$, corresponding to a total volume flow of 2 L/h. The streamlines are highly intertwined in this flow regime, forming curved and tilted lamellae. The voids appearing at the boundary of the mixing channel are due to recirculation zones, which are disconnected from the streams entering the mixer domain.

The streamline pattern of Figure 2d offers an explanation for experimental data obtained with the same flow rates. In the experimental Part I of this article (Hessel et al., 2002) two techniques are presented for characterizing the mixing process in micromixers. The first is based on the diffusion of

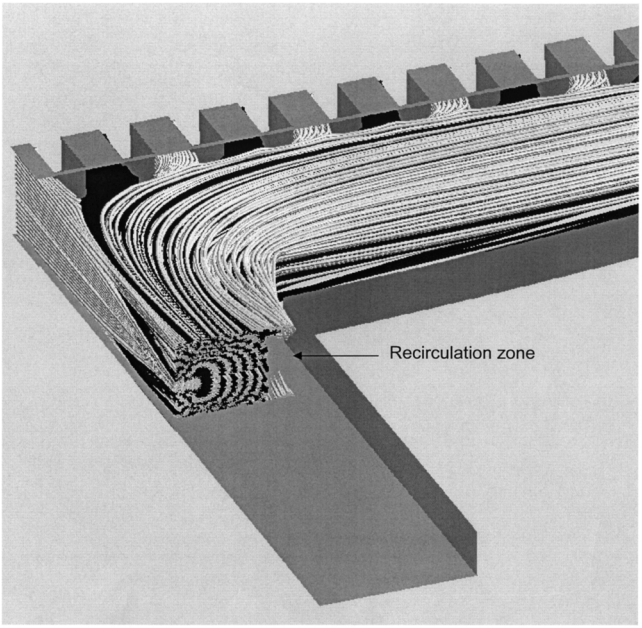

Figure 2d. Streamline pattern in the slit-shaped mixer at *Re* = 2,160.

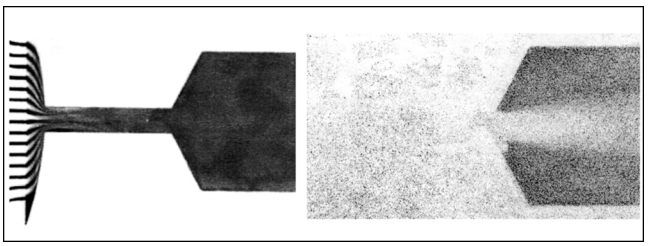

Figure 2e. Characterizing mixing by diffusion of a dye in an aqueous solution (left) and by a chemical reaction yielding a colored complex (right), as described by Hessel et al. (2002).

a dye in an aqueous solution, and the second relies on a chemical reaction yielding a colored complex (rhodanide). The corresponding experimental results are displayed in Figure 2e.

At first glance, the two experimental results seem contradictory. In the lefthand side of the figure, the lamella structure, which is visible in the focusing zone, disappears in the mixing channel, thus suggesting that the fluids have been mixed. However, the righthand side of the figure indicates that, in the mixing channel, conversion to the product does not occur. From the latter, it can be concluded that mixing has not progressed to any substantial degree when the fluids leave the constriction. The streamline patterns displayed in Figure 2d offer an explanation for these results: when light transmits the layered lamella structure in the mixing channel, it intersects both types of lamellae. Thus, an average color is observed, even if no substantial mixing has occurred.

The previous simulation methods aim at characterizing a binary system with a vanishing diffusion constant and providing qualitative information on mixing processes. In order to perform meaningful simulations for small diffusion constants as characteristic for liquids, extreme care has to be taken to define high-quality computational grids aligned with the fluid streamlines. Simulation results for the triangular mixer show that, even in cases where a comparatively fine grid is used and the grid cells are aligned with the flow velocity in most of the domain, numerical diffusion can, generally, not be neglected. As a bulk measure for mixing quality, a quantity r—termed "mixing residual"—is defined as

$$r = \frac{1}{A} \int_S |c(x,t) - 1/2| da \tag{5}$$

where the integral is over the cross-sectional area of the flow domain. With the convention that the unmixed fluids are represented by concentration values of 0 and 1, respectively, r takes a value of 0.5 initially and gets reduced to 0 when complete mixing has occurred. The simulations for the triangular mixer were based on a numerical grid of about 500,000 cells and a total volume flow of 100 mL/h of water, corresponding to a Reynolds number of 108 in the mixing channel. The results are displayed in Figure 2f as the mixing residual as a function of position, where $x = 0$ mm corresponds to the inlet region and $x = 18$ mm to the outlet. At $x = 8$ mm, the focusing zone merges with the actual mixing channel. The fluid streamlines (in white) and the grid cells in the entrance region are shown in the lefthand side of Figure 2f, where one block in the graphical presentation corresponds to 9 grid cells. Two simulations with diffusion constants of $D = 0$ and $D = 10^{-9}$ m^2/s were performed.

The $D = 0$-curve clearly exhibits the effects of flow alignment with respect to grid cells on numerical diffusion. The

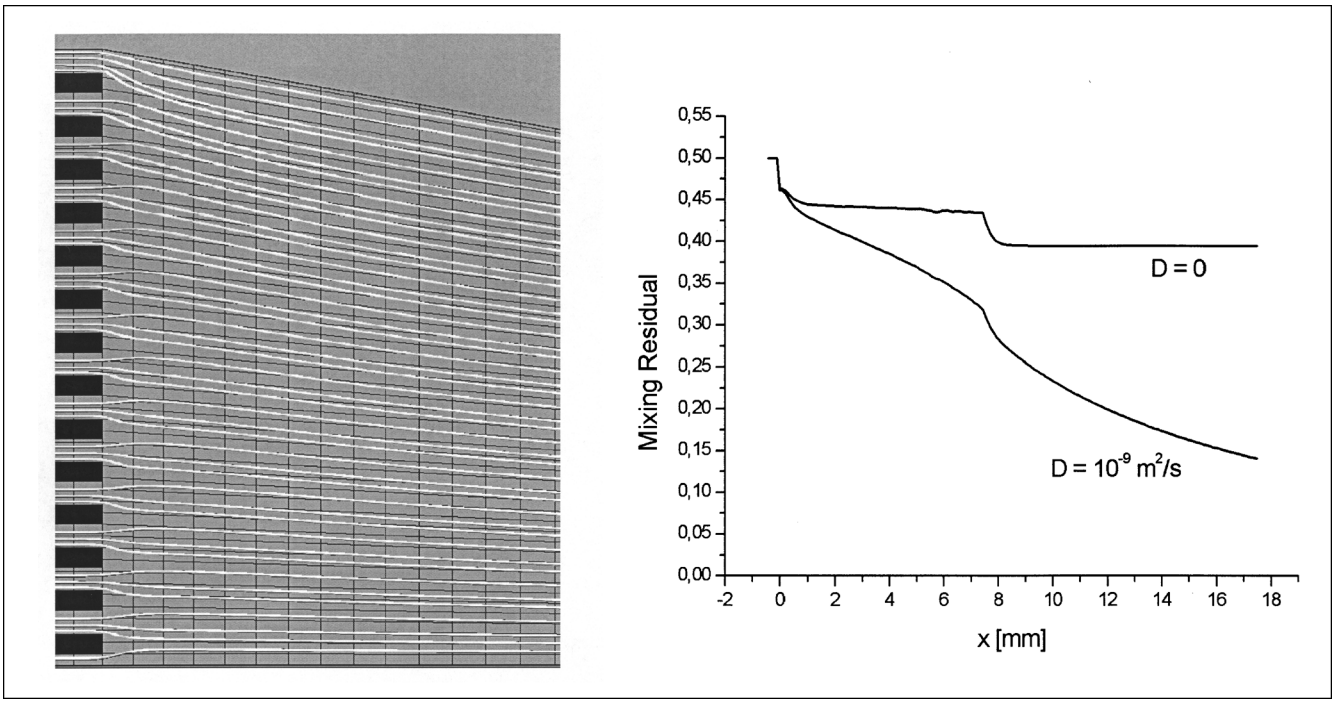

Figure 2f. Streamlines in the inlet region of the triangular mixer and mixing residual as a function of position.

velocity vectors are aligned with the grid cells reasonably well in most of the flow domain with the exception of the inlet region and the interface between the mixing channel and the focusing zone. The corresponding curve of the mixing residual in Figure 2f shows that this suffices to induce sizeable diffusive fluxes. Thus, it becomes obvious that even a very localized misalignment of flow velocity and grid cells can introduce considerable numerical errors, which prevent the quantitative predictions of mixing in microfluidic devices.

Semianalytical Model

To extract some quantitative information on mixing from the computed streamline patterns, the following simplified approach was taken. For all of the mixer geometries presented, mixing mainly occurs in a mixing channel of a rectangular cross-section. In the case of the rectangular and triangular mixers, the flow comprises an interdigital arrangement of fluid lamellae bounded by lateral channel walls. When neglecting the effect of these lateral walls and assuming a constant velocity over the cross section of the mixing channel (which equals the average flow velocity), the mixing process can be described as a pure diffusion problem with periodic boundary conditions. By these means, the complete mixing process can be described by diffusive transport over the domain of a single lamella. Figure 3a illustrates the diffusional dissolution of a liquid lamella, which is described by a concentration profile of an initially rectangular shape. The numbers assigned to the profiles indicate the time at which a curve was computed in units of the diffusion time scale $T = L^2/D$, where L is the lamella width and D is the diffusion constant. For all investigations reported in this section, D was chosen as 10^{-9} m^2/s, a characteristic value for diffusion in liquids.

The underlying mathematical framework allowing the computation of the time evolution of concentration profiles is the diffusion equation, given as

$$\frac{\partial c}{\partial t} = D\,\frac{\partial^2 c}{\partial x^2} \tag{6}$$

where c again denotes the concentration field. Given the invariance of the diffusion equation under inversion of the spatial coordinate and the periodicity of the problem, the solution can be written as a cosine Fourier series

$$c(x,t) = \sum_n c_n(t)\cos(k_n x), \quad k_n = \frac{n\pi}{L}, \quad n = 0,1,2,... \tag{7}$$

Inserting this ansatz into the diffusion Eq. 6, the following solution is obtained

$$c(x,t) = \frac{1}{2} + \sum_{n=1,3,...} \frac{2(-1)^{\frac{n-1}{2}}}{n\pi}\exp\left(-Dk_n^2 t\right)\cos(k_n x) \tag{8}$$

The curves displayed in Figure 3a were obtained by summing up the Fourier series of Eq. 8. In order to compare the performance of different interdigital micromixers, the Fourier series (Eq. 8) was summed up numerically. The triangular

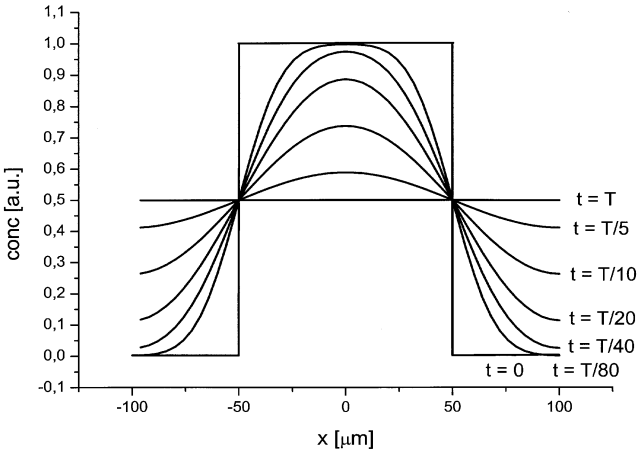

Figure 3a. Dissolution of a rectangular concentration profile.

and slit-shaped micromixers comprise a focusing zone followed by a mixing channel. Due to the comparatively large lamella width, no substantial mixing occurs in the focusing zone for comparatively high volumetric flow rates. For this reason, the focusing zone was neglected and the mixing residual was computed solely on the basis of the mixing channel. Figure 3b shows a comparison between the different types of mixers, with the mixing residual being displayed as a function of time (left) and of length (right). The transformation between time and length was done using the average flow velocities in the mixing channel, where a volume flow of 50 mL/h was assumed for each of the fluids (corresponding to a total volume flow of 100 mL/h). In the case of the rectangular and triangular mixers, the lamella width L in the mixing channel was obtained by equally distributing n inlet streams (n being either 30 or 124) over the width of the channel. A uniform lamella width is supported by CFD simulations for the triangular and rectangular mixers, which show an equidistribution of liquid lamellae over most of the channel width. In the case of the slit-shaped mixer, the lamellae get tilted and assume a nonuniform width, as apparent from Figure 2b. In this case the lamella width L was determined from the central region of the channel where hydrodynamic focusing occurs. In order to account for the higher flow velocity in the central region, the maximum flow velocity in rectangular channels, as obtained from Purday (1949) was used instead of the average flow velocity.

From Figure 3b, it becomes apparent that, with the slit-shaped and SuperFocus mixer, mixing times in the order of ms are achieved. Fast mixing is a prerequisite for many chemical reactions occurring on short time scales (Bourne et al., 1977; Belevi et al., 1981). However, it should be pointed out that, for the slit-shaped mixer, due to the nonuniformity of liquid lamellae, the mixing process will be inhomogeneous, resulting in a varying mixing quality over the channel cross section. When time is translated to distance via the flow velocity in the mixing channel, the advantage of the focusing mixers (triangular and slit-shaped) over the rectangular mixer is less pronounced, but still evident. By focusing a fluid stream to a comparatively narrow mixing channel, the residence time in the mixer decreases. However, this disadvantage is over-

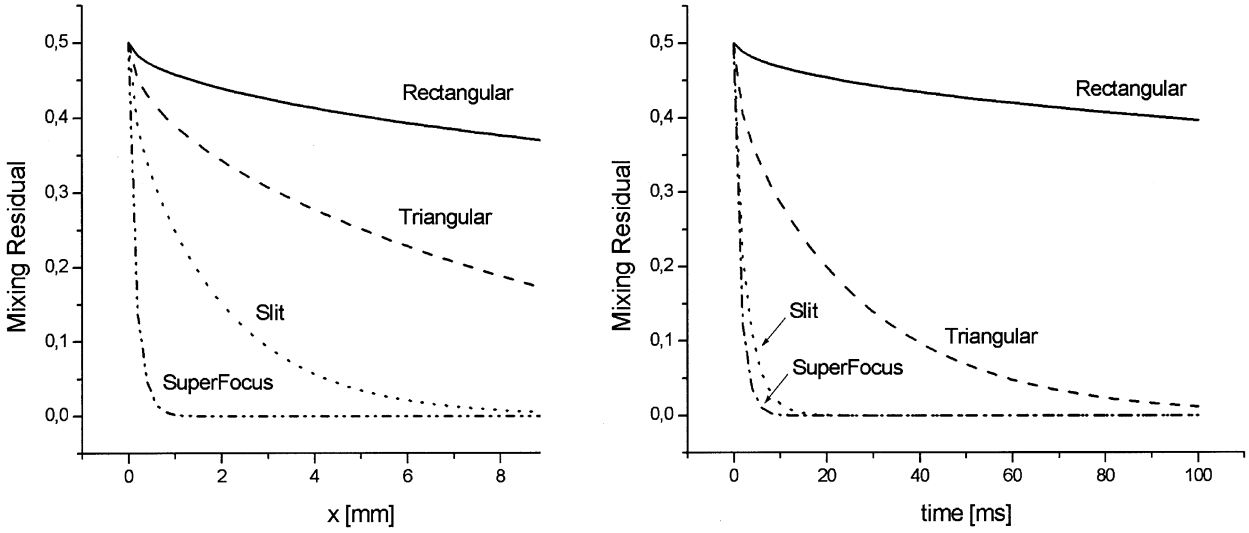

Figure 3b. Mixing residual as a function of distance (left) and time (right).

compensated by the decrease of lamella width. The fact that the diffusion time-scale L^2/D depends *quadratically* on L, whereas the residence time in the mixing channel is a *linear* function of the channel width, makes geometric focusing a powerful method to achieve fast mixing.

When comparing the CFD results and the results from the semi-analytical model for the triangular mixer, values of the outlet mixing residual of comparable magnitude are obtained. At the outlet of the mixing channel, the CFD simulation gives a value of $r = 0.140$, whereas the semi-analytical model yields $r = 0.155$. The CFD results are expected to be lower due to mixing effects in the focusing zone and numerical diffusion.

The model Eq. 8 predicts that, with the SuperFocus mixer, it should be possible to mix liquids even at flow rates of several L/h. Hessel et al. (2002) describe an experiment which allows to assess the mixing process via a binary reaction of two transparent solutions yielding a colored complex. In Figure 3c, an image taken from such an experiment at a total flow rate of 4 L/h is displayed. In contrast to Figure 2e there are no transparent regions in the mixing channel indicating poor mixing, in spite of the flow rate being twice as high. Instead, coloring of the liquid sets is already in the focusing zone. In order to study the progression of mixing, photographic images of the liquid mixture at various positions in the mixing channel were taken with a CCD camera, starting at the interface between the focusing zone and the mixing channel. The images were transformed into grayscale format, where the grayscale level provides information on the average concentration of the colored complex formed in the course of the reaction. However, a simple proportionality between the grayscale level and the product concentration cer-

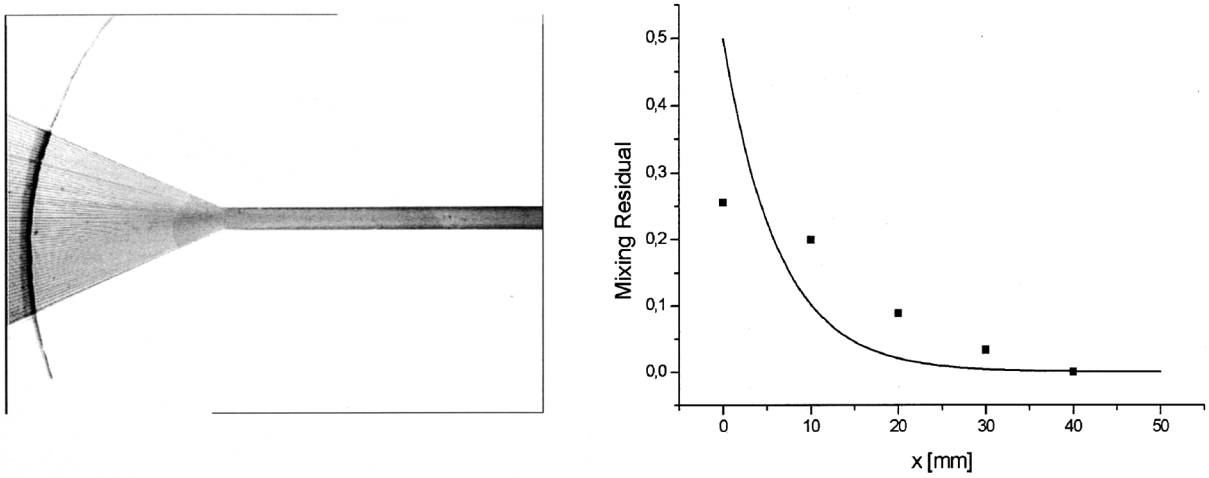

Figure 3c. Characterizing mixing inside the SuperFocus mixer by the reaction described by Hessel et al. (2002) (left) and comparison of experimental (squares) and theoretical (solid line) mixing residuals as a function of the axial position in the mixing channel (right).

The position $x = 0$ corresponds to the interface between focusing zone and mixing channel.

tainly does not exist. Nevertheless, a "mixing residual" was derived from the grayscale level by assigning a value of 0.5 to the transparent liquid, and 0.0 to the tint the liquid assumes asymptotically downstream and interpolating linearly for intermediate values. On the righthand side of Figure 3c, the mixing residual obtained from the grayscale level is compared to the prediction of Eq. 8.

As apparent from the figure, due to mixing in the focusing zone, the experimental numbers start at values substantially lower than 0.5. In the considered case mixing in the focusing zone can obviously not be neglected, as assumed in the model. The figure shows that the experimentally and the theoretically determined mixing residuals follow qualitatively different curves. However, the length scales at which the mixing residuals get reduced to 0 are comparable. As a one-to-one correspondence of experiments and simulations was not expected anyhow due to the nonlinear dependence of the grayscale level on concentration, it can be concluded that the experimental data support the model predictions.

Summary and Conclusions

The flow patterns and mixing properties of various interdigital micromixers were investigated using CFD methods and a semi-analytical model based on the diffusion equation. Even for comparatively fine computational grids of about 500,000 cells, the CFD results displayed numerical artifacts which prevent a quantitative prediction of mixing effects. This statement remains true even when using third-order discretization schemes for the species concentration equation and grid cells aligned with the fluid streamlines in most of the flow domain. As we have shown, even a misalignment in a few cells introduces a considerable amount of numerical diffusion. In order to get some qualitative insight into the mixing mechanisms, streamline integration was employed. By streamline tracking, the geometrical arrangement of liquid lamellae could be displayed, thus revealing effects as lamella tilting or inertial focusing in the slit-shaped mixer. When comparing the computed flow patterns with the experimental results (Hessel et al., 2002), an explanation could be given for contradictory observations at first sight. In a transmitted-light experiment with dyed liquids mixing can be suggested when the light beams intersect layers of different color.

The analytical model developed is based on a Fourier-series type solution of the diffusion equation and can be employed to obtain quantitative information on mixing. The model is valid when the liquid lamellae are equally distributed over the cross-section of the mixing channel. A comparison of the model results for the four different types of micromixers suggests that, with the SuperFocus and the slit-shaped mixer, mixing times in the range of milliseconds are obtained. Such short mixing times provide favorable, well-defined process conditions for fast chemical reactions. When translating mixing times to mixing length scales via the average flow velocity in the devices, the SuperFocus and slit-shaped mixer are still superior to the triangular and rectangular mixer. In this context, the decrease of residence time by geometric focusing (a reduction of the flow cross-section) is overcompensated by the quadratic effects due to a decrease of lamella width. Finally, the prediction for the mixing residuals in the SuperFocus mixer was compared to experimental data stemming from the concentration of a colored complex being formed in a binary chemical reaction. A comparison of the model and experiments suggest similar time scales for mixing and the formation of rhodanide, thus supporting the model predictions.

The results indicate that even in comparatively simple micromixers, quite complex flow patterns may emerge. Therefore, simple experimental methods for characterizing the mixing process (such as dyed solutions) are likely to fail in many cases. Concerning the optimization of micromixing devices and the reduction of mixing times, a clear strategy is suggested by the results of this work: the focusing of many inlet streams to a narrow mixing channel.

Literature Cited

Belevi, H., J. R. Bourne, and P. Rys, "Chemical Delectivities Disguised by Mass Diffusion. VII. A Simple Model of pH-Dependence of Product Distribution in Mixing-Disguised Azo Coupling Reactions" *Helv. Chim. Acta*, **64**, 1599 (1981).

Bessoth, F. G., A. deMello, and A. Manz, "Microstructure for Efficient Continuous Flow Mixing," *Analytical Communications*, **36**, 213 (1999).

Bourne, J. R., E. Crivelli, and P. Rys, "Chemical Selectivities by Mass Diffusion. V. Mixing-Disguised Azo Coupling Reactions," *Helv. Chim. Acta*, **60**, 2944 (1977).

Ehrfeld, W., K. Golbig, V. Hessel, H. Löwe, and T. Richter, "Characterization of Mixing in Micromixers by a Test Reaction: Single Mixing Units and Mixer Arrays," *Ind. Eng. Chem. Res.*, **38**, 1075 (1999).

Ehrfeld, W., V. Hessel, and H Löwe, *Microreactors*, Wiley-VCH, Weinheim (2000).

Herweck, T., S. Hardt, and V. Hessel, "Visualization of Flow Patterns and Chemical Synthesis in Transparent Micromixers," *Proc. Int. Conf. on Microreaction Technol., IMRET* 5, Strasbourg (May 27-30, 2001).

Hessel V., S. Hardt, H. Löwe, and F. Schönfeld, "Laminar Mixing in Different Interdigital Micromixers: I. Experimental Characterization," *AIChE J.*, **49**, 566 (2003).

Leonard, B. P., "Locally Modified QUICK Scheme for Highly Convective 2D and 3D Flows," *Proc. Int. Conf. on Numerical Methods in Laminar and Turbulent Flow*, Part 1, Pineridge Press, Swansea (1987).

Noll, B., *Numerische Strömungsmechanik*, Springer, Berlin (1993).

Purday, H. F. P., *An Introduction to the Mechanics of Viscous Flow*, Dover, New York (1949).

van Doormal, J. P., and G. D. Raithby, "Enhancement of the SIMPLE Method for Predicting Incompressible Fluid Flows," *Numerical Heat Transfer*, **7**, 147 (1984).

Manuscript received Feb. 7, 2002, and revision received Oct. 11, 2002.